

A study of the AgBr(111) and AgBr(100) surface by means of atomic force microscopy

E. Meyer, H. Heinzelmann, P. Grütter, H.-R. Hidber, H.-J. Güntherodt, and R. Steiger

Citation: [Journal of Applied Physics](#) **66**, 4243 (1989); doi: 10.1063/1.343964

View online: <http://dx.doi.org/10.1063/1.343964>

View Table of Contents: <http://scitation.aip.org/content/aip/journal/jap/66/9?ver=pdfcov>

Published by the [AIP Publishing](#)

Articles you may be interested in

[Scanning tunneling microscopy studies of thin film AgBr on Au\(111\)](#)

J. Vac. Sci. Technol. A **12**, 2023 (1994); 10.1116/1.579000

[Friction force microscopy on clean surfaces of NaCl, NaF, and AgBr](#)

J. Vac. Sci. Technol. B **12**, 2227 (1994); 10.1116/1.587747

[Effect of adsorbed species on the surface potential of AgBr](#)

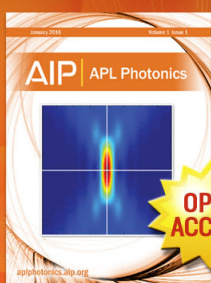
J. Appl. Phys. **53**, 4289 (1982); 10.1063/1.331258

[Model for surface diffusion in AgBr](#)

J. Appl. Phys. **46**, 469 (1975); 10.1063/1.321364

[Surface Structures and Epitaxial Growths on AgBr Microcrystals](#)

J. Appl. Phys. **35**, 2165 (1964); 10.1063/1.1702810



Launching in 2016!

The future of applied photonics research is here

AIP | APL
Photonics

A study of the AgBr(111) and AgBr(100) surface by means of atomic force microscopy

E. Meyer, H. Heinzelmann, P. Grütter, H.-R. Hidber, and H.-J. Güntherodt
Institut für Physik, Klingelbergstrasse 82, CH-4056 Basel, Switzerland

R. Steiger
Ilford AG, CH-1700 Fribourg, Switzerland

(Received 12 April 1989; accepted for publication 26 June 1989)

For the first time, atomic force microscope measurements on the (111) and (100) surfaces of AgBr crystals are reported. We could image steps of varying sizes ranging from 0.9 nm to several nm. The lateral orientation of these steps could be determined by comparison with x-ray measurements. On the (100) surface, steps with the low index orientations $\langle 01\bar{1} \rangle$ and $\langle 011 \rangle$ were observed. On the (111), surface steps were mainly oriented in the $\langle \bar{1}21 \rangle$ and $\langle 1\bar{1}0 \rangle$ directions. The most evident difference between these surfaces was that on the (111) surface no crossing steps occurred. This observation will be discussed in relation to the adsorption of dye aggregates on these crystals, which is of great importance for photographic emulsion technology.

I. INTRODUCTION

According to a recent review by Hamilton,¹ the primary photographic process is strongly influenced by certain surface properties of the silver halides. Kink sites on the surface and jogs on dislocations are regarded as sinks and sources for defects (silver-ion interstitials Ag_i^+ and silver-ion vacancies). Actually, it is known that the surface generation process is dominant in silver halide microcrystals with respect to the Frenkel mechanism. For a $0.1\text{-}\mu\text{m}^3$ AgBr microcrystal, one pair of defects is attributed due to the Frenkel equilibrium, and 10^3 or more Ag_i^+ will be surface induced. Besides the production of interstitials, partially charged kink sites and jogs play a crucial role in the nucleation and growth of silver clusters forming the latent image. According to the Gurney-Mott principle,² the absorbed photon produces an electron-hole-pair. If the electron is trapped, it is probable that this electron combines with a mobile Ag_i^+ . If the trapping center is close to a positive kink site or jog, the net partial charge of $-e/2$ leads to a coulombic attraction of a Ag_i^+ . Further absorption of a photon, trapping of the electron, and attraction of the silver ion will lead to the growth of a silver cluster. The partial charge will promote this growth until the cluster is stable enough to act as a latent image.

Silver halide monocrystals were shown^{3,5} to represent a good model for studies of the photographic process. After exposure to actinic light, half-tone images can be developed in a chemical or a physical developer. Kanzaki⁵ has shown by the observation of printout silver that silver centers form at the surface and not in the subsurface region, where the Ag_i^+ concentration is high. This is a strong indication that kink sites are nucleation centers for silver clusters. Although there is much evidence for this concept, there are still open questions. Classical kink sites are located on the (100) surface of ionic crystals. On the (111) surface, there is no strict analogy to these kink sites. The presence of similar, partially charged "kinklike" sites is only presumed. A further question is the nature of the reconstruction of the AgBr (111) being necessary for charge neutrality.

In this context, it is clear that the surface structure is of great interest. To our knowledge, the only technique applied systematically to investigate the silver halide surface structure is metal decoration combined with scanning electron microscopy. Hamilton and Brady^{6,7} found preferential sites forming an ordered array and proposed several possible structural models for the (111) surface. They could not observe steps or kinklike sites.

The recently developed atomic force microscope (AFM)⁸ is a method to investigate the local structure of insulating surfaces. Similar to the stylus profilometer, a force sensor is raster scanned nearby the surface. With a high sensitivity of about 0.01 \AA , the interaction force is monitored by the measurement of the deflection of a cantilever-type spring. Typical interaction forces range between 10^{-6} and 10^{-11} N .⁹ Several layered compounds as highly oriented pyrolytic graphite and highly oriented pyrolytic boron nitride and MoS_2 ¹⁰⁻¹³ could be imaged with atomic resolution. The application to the ionic crystal LiF has been reported in a previous work.¹³ Steps of one cell height have been imaged. The present paper is the first systematic AFM study on the AgBr surface. We investigated the (100) and (111) surface of AgBr monocrystals. The local step structure could be resolved. Step heights and lateral orientations with respect to the bulk lattice were determined. Distinct differences between the step structure on the (100) and (111) were found. These results will be discussed with respect to the preferential growth of dye aggregates on these surfaces. Atomic resolution has not yet been achieved.

II. EXPERIMENT

A. Sample preparation and characterization

With a crucible-free method,¹⁴ single crystals of high purity have been prepared. A 99.9995% Ag rod was heated with a frequency coil to 600°C . In the presence of a bromine atmosphere (200 Torr), the AgBr single crystal was grown. The total impurity content was determined to be less than 1 ppm, which corresponds to the purest monocrystals ever re-

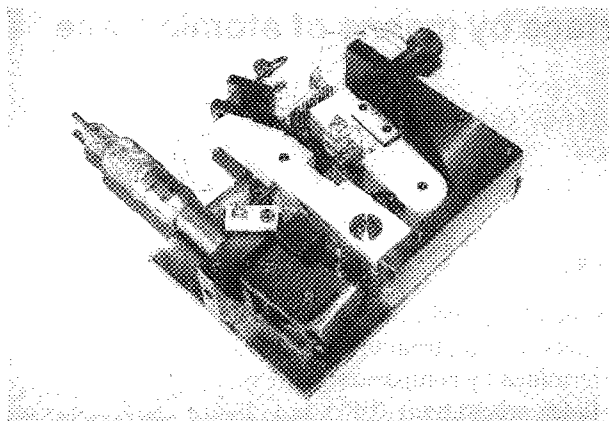


FIG. 1. Photograph of our instrument. From the left to the right are the micrometric screw, the eccentric mechanism, the block of ceramics with the STM and the leaf spring, the block with the sample, and the coarse screw. The support of the cantilever is directly mounted to the leaf spring with a magnet or glue.

ported in the literature. A chemical polishing method has been applied to obtain a minimum surface roughness.³

It was shown with Rutherford backscattering spectroscopy that the crystal is well ordered up to at least two to three layers below the surface.¹⁵ From scanning electron microscopy and optical interference microscopy, we concluded that the mean surface roughness is below 30 nm. Ellipsometry confirmed that the crystals are contamination free. No adsorbed silver-cyano complexes from chemical polishing with KCN are present at the surface. AgBr surfaces are known to be inert in air. Water films do not absorb (ellipsometer measurements). For AFM measurements, samples were cut from the AgBr rod after x-ray orientation. Caution

was taken to avoid contact with metals, which would lead to corrosion of the samples. All measurements have been performed under red light. Actually, one of the major advantages of the AFM is that any exposure to actinic radiation can be avoided.

B. Instrumentation

The instrument is mounted on a commercial antivibration table and is operated in ambient air. The deflection of the cantilever is monitored with electron tunneling. For this reason, a scanning tunneling microscope (STM) device is fixed to a ceramic block (cf. Fig. 1). The cantilever support is attached to a leaf spring. With two screws the leaf spring can be bent, leading to a well-defined approach of the lever to the STM tip. STM and cantilever together act as the force sensor. This sensor is approached to the sample with a combination of micrometric screw and eccentric mechanism. This way small, controlled movements of 5 nm can be made.

All movable parts are pressed against hard springs, raising the stiffness of the instrument. We used SiO_2 cantilevers produced by microfabrication.^{10,11} Owing to the small dimensions of the cantilevers ($1.5 \times 40 \times 140 \mu\text{m}^3$), a spring constant of 0.7 N/m can be combined with the high resonance frequency of 63 kHz. The high resonance frequency of the whole system including the cantilever is important to get insensitive to mechanical vibrations of the building and acoustic noise.¹⁶ The choice of machinable ceramics is justified by the similar thermal expansion coefficients of ceramics and piezomaterial leading to small thermal paths, and thus high stability of the tunneling gap and the interaction distance between probing tip and sample.

One severe problem in atomic force microscopy is tip conditioning. At present, microfabrication technique is not able to add a sharp tip to the rectangular or triangular cantilevers. The experimentalist has the choice to use an edge of

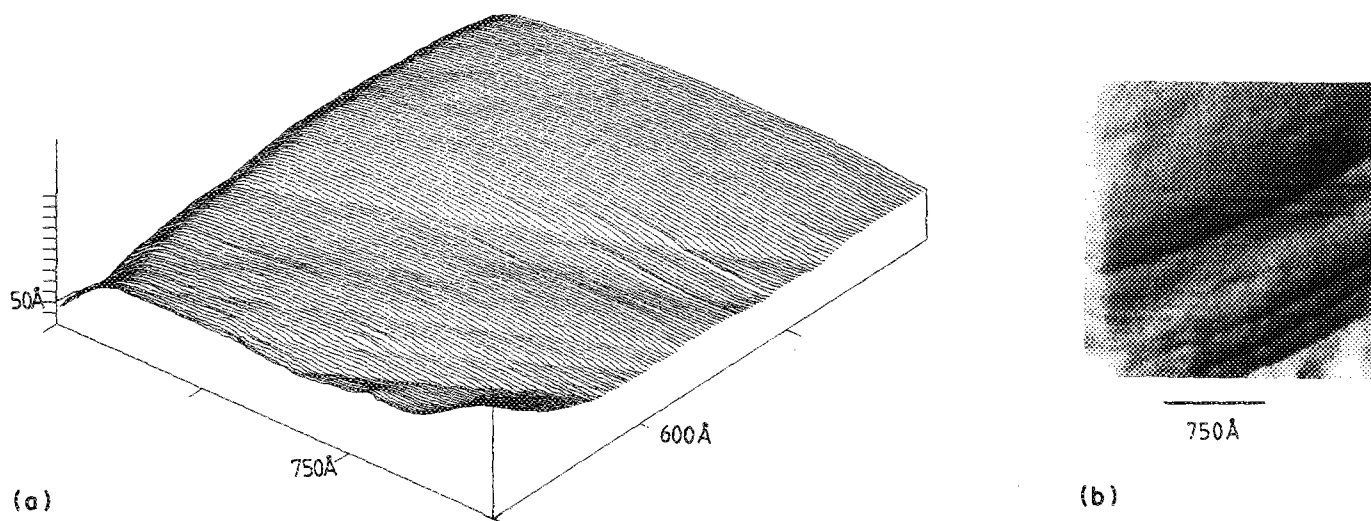


FIG. 2. (a) 1800×2250 -Å line-scan image of AgBr(111). The step height varies between 9 and 28 Å. The step direction corresponds to $[\bar{1}21]$. (b) Bird view of the same measurement. With the help of computer modeling, the surface can be illuminated by an imaginary light source.



(a) 750 Å

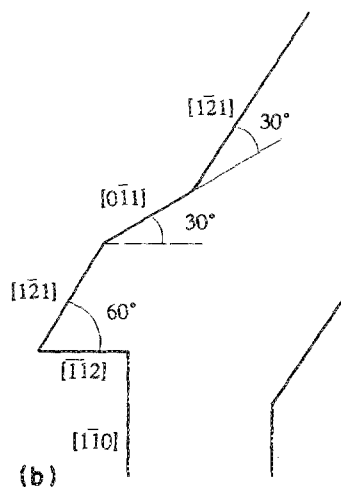


FIG. 3. (a) $1800 \times 2250 \text{ Å}^2$ area of AgBr(111). Starting from the upper right to the lower left, a step changes its direction from $[1\bar{2}1]$ to the $[0\bar{1}1]$, returning again to the $[1\bar{2}1]$, changing to the $[1\bar{1}2]$, and extending finally in the $[1\bar{1}0]$ direction. (b) Schematic diagram showing the step orientation.

the cantilever by tilting the lever or to glue small diamond fragments to the end of the lever. Although the second method needs some manual skill, it turned out to be favorable to minimize multiple tip effects. Scanning electron microscopy studies of such levers showed that the tip radii are in the range of less than 1000 Å . The end of the diamond is formed by a tetrahedron confined by crystallographic faces.

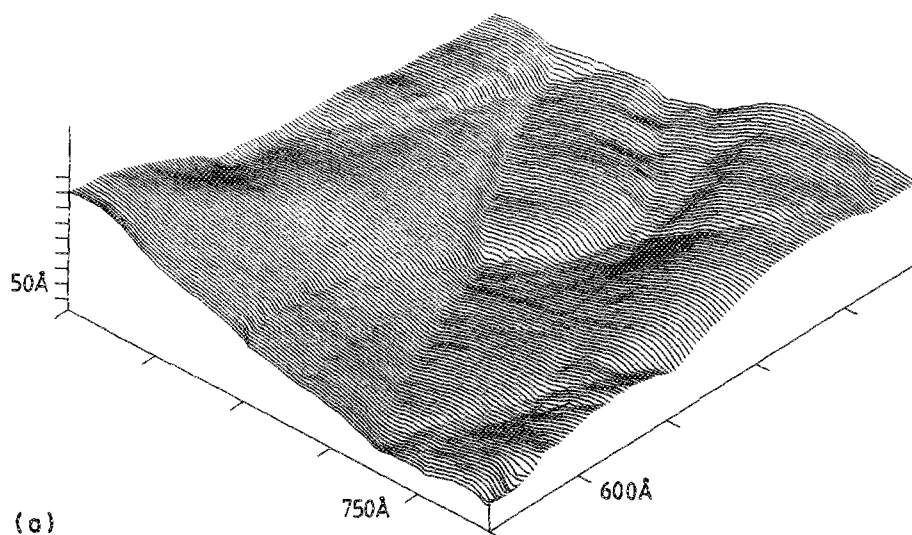
III. RESULTS

Figures 2–5 are examples of the measurements of AgBr. The typical force between probing tip and samples was set repulsive ranging between 10^{-8} and 10^{-7} N . Successive images were very reproducible and revealed small thermal drifts of about 100 Å/h in the lateral direction. The typical time to acquire one image was 1–5 min. Therefore, distortions due to thermal drift can be neglected.

Determining the angle of the steps relative to the crystallographic axes, the different calibration of the piezoscanner has to be taken into account. The accuracy of the angle is about 8° .

Figure 2 is a $1800 \times 2250 \text{ Å}^2$ area of the AgBr(111) surface. The width of the terraces is a few hundreds of Å and the height ranges from 9 to 28 Å . The steps are quite parallel. The orientation is attributed to the $[1\bar{2}1]$. On different locations of the sample, other steps in the $[1\bar{1}0]$ directions were found. An interesting feature is shown in Fig. 3. Here a step changes its direction. Starting from the upper right to the lower left, the $[1\bar{2}1]$ turns into $[0\bar{1}1]$, returns to $[1\bar{2}1]$, changes to $[1\bar{1}2]$, and finally extends in the $[1\bar{1}0]$ direction.

All the steps we could image on the (111) surface were well separated by large terraces. In contrast to this is the behavior on the (100) surface. As shown in Fig. 4, the steps cross each other and the terraces are surrounded by steps. The step heights vary from 10 to 80 Å . The orientation of the



(a)



(b)

FIG. 4. (a) $3000 \times 3750 \text{ Å}^2$ line-scan image of AgBr(100). The steps cross each other. Some curvature of the steps is visible. Thus the crystallographic directions cannot be attributed unequivocally. (b) Corresponding bird view.

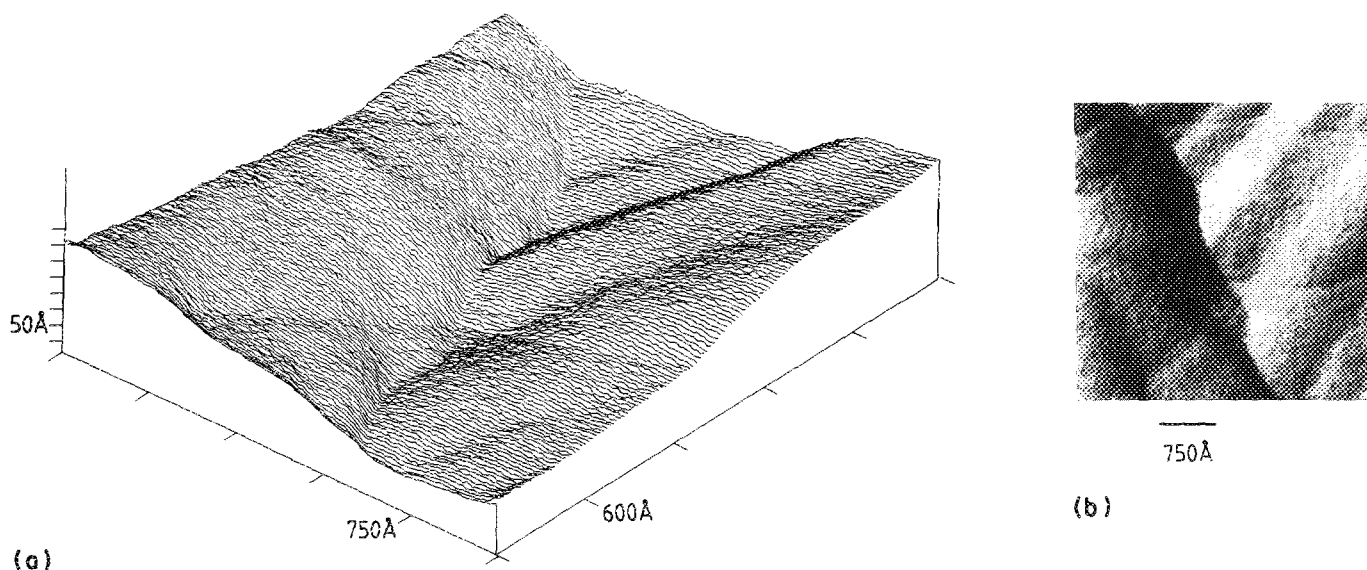


FIG. 5. (a) $3000 \times 3750\text{-}\text{\AA}^2$ line-scan image of AgBr(100). The steps running diagonally can be attributed to $[\bar{1}\bar{1}0]$ and $[110]$. (b) Corresponding bird view.

steps on the (100) was not as conclusive as in the case of the (111). We observe a slight curvature of the steps as shown in Fig. 4. However, in many images the steps aligned in the $[011]$ and $[0\bar{1}1]$ direction. Figure 5 is an example for this.

The measurements on these two faces of AgBr have been performed with different tips. The results were consistent, and multiple-tip effects could thus be excluded. The highest resolution we could achieve is shown in Fig. 6. The step height is $9 \pm 1\text{ \AA}$. With an interreticular distance of 5.77 \AA (unit cell), this corresponds to about two unit cells in AgBr.¹⁷ The step profile is not uniform, but exhibits some substructure. At present it cannot be excluded that this substructure is due to the roughness of the probing tip or due to some adsorbates localized at these steps. The atomic lattice could not be resolved until now. Possible reasons are poor tip conditioning or bad signal-to-noise ratio. Future work will tend to clarify this point.

IV. DISCUSSION

AFM is the only technique by which terraces and steps of atomic dimensions were detected on AgBr surfaces. Such structures could not be revealed by vacuum deposition of metallic nuclei on the (111) faces of epitaxial AgBr films, although it was assumed from this study^{6,7} that the highly ordered metallic nuclei were formed at preferential surface sites of unidentified character. The size and the concentration of platinum-palladium particles deposited on AgBr (111) surfaces were found to be influenced by the presence of an adsorbed cyanine dye forming highly ordered aggregates (so-called *J* aggregates). The resulting appearance of patchlike deposition of the metal particles suggest that certain high-energy surfaces sites were blocked preferentially by dye adsorption. However, no information about the existence of steps and discontinuities was obtained from these studies.⁷

AFM has revealed the structure of surface terraces and steps even at the surface of optimally polished AgBr monocrystals. Rutherford backscattering spectroscopy¹⁵ performed on identically prepared AgBr crystal surfaces showed that the crystal is well ordered up to at least two to three layers below the surface.

The presence of steps on the (111) surface and the changes of their orientation support the existence of the presumed "kinklike" sites. A quantitative comparison will need higher resolution of the step structure. A fundamental difference was found between the (111) and (100) faces, the possible consequences of which will be discussed.

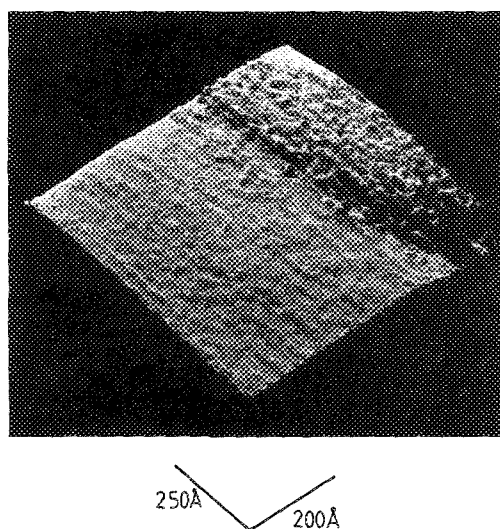


FIG. 6. $600 \times 750\text{-}\text{\AA}^2$ area of AgBr(100). The step is $9 \pm 1\text{ \AA}$ high. The origin of the substructure in the step region is not clear.

AFM has shown that no crossing of steps is observed on the (111) face of AgBr, whereas on the (100) face the steps cross each other very often, which leads to smaller ordered surface domains. It is known¹⁸ that aggregating cyanine dyes are used to modify the crystal growth of silver halides. These molecules inhibit only the octahedral (111) faces of AgBr from random overgrowth by silver chloride, which then occurs on the other sites of the grain.¹⁸ The action of these dye aggregates, so-called "site directors," is probably due to the fact that such aggregation takes place preferentially on those faces where large, two-dimensional dye crystals can grow epitaxially, i.e., on (111) faces of AgBr. On (100) faces, the dimensions of ordered dye aggregates must be smaller, and aggregation occurs in at least two crystallographic directions. The mechanism of dye aggregate formation of AgBr surfaces may be the following: Nucleation for the formation of ordered *J* aggregates occurs within 20 ms after addition of the dye solution to the silver halide.¹⁹ This nucleation probably starts at sites of highest surface energy, i.e., at the steps on the terraced AgBr surface.¹⁷ The growth into a larger dye aggregate is diffusion controlled and takes a minimum time of a few tenths of a second until an aggregate with a certain stability is formed.^{20,21} A highly stable, two-dimensional dye crystal which may attain dimensions up to 100 μm (Ref. 22) is formed after adsorption times of the order of 60 min.²¹ Such dye aggregates have been studied by electron diffraction and synchrotron radiation. They were shown to exhibit a brickstonelike arrangement of the dye chromophores.²² The structure of octahedral AgBr surfaces is still unknown. A comparison of our AFM results with different models proposed by Hamilton and Brady⁶ or by Baetzold, Tau, and Tasker²³ is difficult because of the large uncertainties mentioned above. A conclusive answer to this question can only be given if atomic resolution is achieved. This is the purpose of further AFM studies on AgBr crystal surfaces.

In summary, we have shown that AFM is able to resolve the step structure of AgBr monocrystals. The orientation of the steps coincide with low index orientations. On the (111) face, the $\langle 1\bar{2}1 \rangle$ and the $\langle 1\bar{1}0 \rangle$ directions of the steps are predominant. Changes in step orientations have been observed. The steps are found to be well separated by terraces, whereas in the case of (100) face crossing steps were found very often. On the (100) surface, the correspondence of the steps to certain directions was not as definite as on (111), but a preference of $\langle 110 \rangle$ and $\langle 1\bar{1}0 \rangle$ was found. These results

may help to understand the growth of dye aggregates on AgBr being important for spectral sensitization. Finally, some indications about the origin of "kinklike" sites on the (111) were found.

ACKNOWLEDGMENTS

We wish to thank P. Junod (Ciba-Geigy Ltd.) for supplying us a silver bromide monocrystal of highest purity and J. Ketterer for x-ray diffraction measurements, and R. Buser and N. DeRooij (Institut de Microtechnique, Neuchâtel) for the production of the SiO_2 levers. This work was supported by Swiss National Science Foundation and the Kommission zur Förderung der wissenschaftlichen Forschung.

- ¹J. F. Hamilton, *Adv. Phys.* **37**, 359 (1988).
- ²R. W. Gurney and N. F. Mott, *Proc. R. Soc. London A* **164**, 151 (1938).
- ³R. Steiger, H. Hediger, P. Junod, H. Kuhn, and D. Möbius, *Photogr. Sci. Eng.* **24**, 185 (1980).
- ⁴P. Junod, H. Hediger, B. Kilchör, and R. Steiger, *Photogr. Sci. Eng.* **23**, 266 (1979).
- ⁵H. Kanzaki, *Phys. Rev.* **99**, 1888 (1955).
- ⁶J. F. Hamilton and L. E. Brady, *Surf. Sci.* **23**, 389 (1970).
- ⁷L. E. Brady and J. F. Hamilton, *Photogr. Sci. Eng.* **15**, 138 (1971).
- ⁸G. Binnig, C. F. Quate, and Ch. Gerber, *Phys. Rev. Lett.* **56**, 930 (1986).
- ⁹Y. Martin, C. C. Williams, and H. K. Wickramasinghe, *J. Appl. Phys.* **61**, 4723 (1987).
- ¹⁰G. Binnig, Ch. Gerber, E. Stoll, T. R. Albrecht, and C. F. Quate, *Eur.ophys. Lett.* **3**, 1281 (1987).
- ¹¹T. R. Albrecht and C. F. Quate, *J. Vac. Sci. Technol. A* **6**, 271 (1988).
- ¹²O. Marti, B. Drake, S. Gould, and P. K. Hansma, *J. Vac. Sci. Technol. A* **6**, 287 (1988).
- ¹³E. Meyer, H. Heinzelmann, P. Grütter, Th. Jung, Th. Weisskopf, H.-R. Hidber, R. Lapka, H. Rudin, and H.-J. Güntherodt, *J. Microsc.* **152**, 269 (1988).
- ¹⁴P. Junod, B. Kilchör, and H. Walliser, *J. Cryst. Growth* **10**, 144 (1971).
- ¹⁵M. Roulet, H. Huber, and C. Jaccard, *Phys. Status Solidi A* **35**, 97 (1976).
- ¹⁶D. W. Pohl, *IBM J. Res. Dev.* **30**, 417 (1986).
- ¹⁷H. Wagner, in *Solid Surface Physics*, Vol. 85 of *Springer Tracts in Modern Physics*, edited by J. Hoelzl, F. K. Schulte, and H. Wagner (Springer, New York, 1979), p. 151.
- ¹⁸J. E. Maskasky, *J. Imag. Sci.* **32**, 160 (1988).
- ¹⁹T. Tanaka and M. Iwasaki, *J. Soc. Photogr. Sci. Technol. Jpn.* **50**, 274 (1987).
- ²⁰H. Kuhn, in *Modern Trends of Colloid Science in Chemistry and Biology* (Birkhäuser, Basel, 1979), p. 97.
- ²¹R. Steiger and F. Zbinden, *J. Imag. Sci.* **32**, 64 (1988).
- ²²C. Duschl, W. Frey, Ch. Heim, J. Als-Nielsen, H. Möhwald, and W. Knoll, *Thin Solid Films* **159**, 379 (1988); C. Duschl, W. Frey, and W. Knoll, *Thin Solid Films* **160**, 251 (1988).
- ²³R. C. Baetzold, Y. T. Tan, and P. W. Tasker, *Surf. Sci.* **195**, 579 (1988).